Pre-print of

BERRA F & FELLETTI F. (2011) - *Syndepositional tectonics recorded by soft-sediment deformation and liquefaction structures(continental Lower Permian sediments, Southern Alps, Northern Italy): Stratigraphic significance*. Sediment. Geol. 235, 249-263.

Syndepositional tectonics recorded by soft-sediment deformation and liquefaction structures (continental Lower Permian sediments, Southern Alps, Northern Italy): stratigraphic significance

F. Berra and F. Felletti

Università degli Studi di Milano – Dipartimento Scienze della Terra, via Mangiagalli 34, 20133 I-Milano

Corresponding Author: Fabrizio Berra. Università degli Studi di Milano, Dipartimento di Scienze della Terra,Via Mangiagalli, 34 , 20133 Milano, Italy. Tel. ++39 02 503 15498. E-mail: fabrizio.berra@unimi.it

Abstract

The Lower Permian succession of the Central Southern Alps (Lombardy, Northern Italy) was deposited in fault-controlled continental basins, probably related to transtensional tectonics. We focussed our study on the stratigraphic record of the Lower Permian Orobic Basin, which consists of a 1000 m thick succession of prevailing continental clastics with intercalations of ignimbritic flows and tuffs (Pizzo del Diavolo Formation, PDV) resting on the underlying prevailing pyroclastic flows of the Cabianca Volcanite. The PDV consists of a lower part (composed of conglomerates passing laterally to sandstones and distally to silt and shales), a middle part (pelitic, with carbonates) and an upper part (alternating sandstone, silt and volcanic flows). Syndepositional tectonics during the deposition of the PDV is recorded by facies distribution, thickness changes and by the presence of deformation and liquefaction structures interpreted as seismites. Deformation is recorded by both ductile structures (ball-and-pillow, plastic intrusion, disturbed lamination, convolute stratification and slumps) and brittle structures (sand dykes and autoclastic breccias). Both the sedimentological features and the geodynamic setting of the depositional basin confidently

support the interpretation of the described deformation features as related to seismic shocks. The most significant seismically-induced deformation is represented by a slumped horizon (about 4 m thick on average) which can be followed laterally for more than 5 km. The slumped bed consists of playa-lake deposits (alternating pelites and microbial carbonates, associated with mud cracks and vertebrate tracks). The lateral continuity and the evidence of deposition on a very low-angle surface along with the deformation/liquefaction of the sediments suggest that the slump was triggered by a high-magnitude earthquake.
The stratigraphic distribution of the seismites allows us to identify time intervals of intense seismic activity, which correspond to rapid and basin-wide changes in the stratigraphical architecture of the depositional basin and/or to the reprise of the volcanic activity.
The nature of the structures and their distribution suggest that the magnitude of the earthquakes responsible for the observed structures was likely higher than 5 (in order to produce sediment liquefaction) and probably reached intensity as high as 7 or more. The basin architecture suggests that the foci of these earthquakes were located close to the fault-controlled borders of the basin or within the basin itself.

Keywords: Early Permian, syndepositional tectonics, Southern Alps, sediment liquefaction, seismites
Running title: Early Permian seismically-induced deformation, Southern Alps

1 - Introduction

Layered heterolithic sediments are often affected by early deformation, which may develop when the sediments are still unconsolidated or partly cohesive. Deformation of sediments generally occurs on the exposed surface or in the immediate subsurface in subaerial/subaqueous conditions and in the presence of low-permeability beds capping water-saturated sediments.
Soft-sediment deformation and liquefaction are processes which require the complete saturation of the sediments by surface water (i.e. water-filled ponds/basins such as lakes) or water table. The development of deformation is related to the physical properties of the sediments (mainly grain size) which control the porosity/permeability of the sediment and its cohesion.

The triggering factors which control the deformation of soft or partly-consolidated sediment can be ascribed to slope instability, to loading of sediments and escape of water or to shaking of sediment due to seismic activity. These different factors can often produce similar structures, but some characteristics can be extremely useful to identify the origin of sediment deformation (Moretti and Sabato, 2007). Soft-sediment deformation structures are more ambiguous, whereas liquefaction is predominantly related to seismic shocks, mainly because cyclic shear waves have the capability to increase pore-water pressures (in water-saturated sediments) and change the state of a sediment from solid-like to viscous liquid-like material (Obermeier; 1996a). The transition from solid to viscous state can trigger fluidization of sediments close to the depositional surface but also sediment failures with the development of slump overfolds (Allen, 1982) even on low-angle slopes (Field et al., 1982). Tectonically active sedimentary basins may preserve seismically induced structures, mainly in sandy-silty sediments saturated with water, where the clay content is less than 15%.

The distribution, nature and intensity of seismically induced deformation are also controlled by the magnitude of the earthquakes. Seismically-induced deformation/liquefaction has been recognized associated with historical earthquakes (Obermeier, 1996a and references therein) as well as in older sediments (e.g. Rodriguez-Pascua et al., 2000). Data on the intensity of the earthquakes and their effects on sediments suggest that liquefaction is generally produced when magnitude is greater than 5.0/5.5 (Atkinson, 1984; Galli, 2000).

The occurrence of soft-sediment deformation and liquefaction in sediments which do not commonly present such structures in aseismic settings, deposition in fault-controlled basins and the abundance and lateral continuity of the deformed layers (Obermeier, 1996a) can be considered the best evidence of a strong seismic overprint on the original sedimentary succession. All these requirements are present in the Lower Permian succession of the Southern Alps of Italy, which consists of a thick, coarse to fine grained continental succession, where different types of sediment deformation and liquefaction structures are common. The description and interpretation of these structures along with the significance of their stratigraphic distribution (with respect to major changes in the stratigraphic architecture of the sedimentary succession) is the main focus of this work.

2 - Geological setting

After the Variscan orogeny, the future alpine area was characterized during the Early Permian by the development of fault-controlled basins where thick successions of pyroclastic and lava flows

alternating with continental clastics were deposited (Fig. 1). Widespread calcalkaline magmatism and extensional (probably transtensional) tectonics characterized large parts of the future alpine area and surrounding domains. Continental basins with important volcanic supply and syndepositional tectonics are presently preserved throughout southwestern Europe: Spain, southern France (i.e. Gand and Durand, 2006), Corsica and Sardinia, northern Apennine and Southern Alps (i.e. Virgili et al., 2006 and references therein). In the Southern Alps, beside the effusive volcanic activity, Early Permian intrusive events at different crustal depth (i.e. Ivrea Verbano body, Laghi Granites) confirm major volcanic activity along the Variscan suture, lasting about 20 Ma (Peressini et al., 2007).

In the Southern Alps, along an east-west section, it is possible to recognize different Early Permian successions (from west, Fig. 1): the Biella Volcanics, the Varese-Lugano District, the Orobic Basin, the Collio Basin, the Tione Basin, the Tregiovo Basin, the Atesinian District and the Pramollo Basin (Cassinis et al. 1988). These successions are characterized by different depositional architectures. Some basins (i.e. Atesinian District) are characterized by a prevalence of volcanic (ignimbrite) deposits; others (Collio Basin, Tregiovo Basin) are characterized by different pulses of volcanic activity alternating with periods of siliciclastic sedimentation; others (Orobic Basin) consist of a prevalent volcanic succession covered by prevailing sedimentary units. The maximum thickness of sediments and volcanites reaches 4 km, and the size of each single basin is up to several hundreds of square kilometres (Fig. 1). The transtensional tectonics responsible for the development of the Permian basins and related volcanic activity has been attributed to: 1) late Variscan dextral wrenching which affected large parts of southern Europe (e.g., Arthaud and Matte, 1977; Schaltegger and Brack, 2007); 2) post-collisional collapse of the Variscan belt (Malaveille et al., 1990); 3) the initial stages of Tethyan rifting (e.g., Winterer and Bosellini, 1981; Siletto et al., 1993); 4) backarc basin development in the hangingwall of a West-directed subduction zone affecting the underlying Hercynian-Variscan orogen (Doglioni, 1995).

The Orobic Basin is one of the largest Permian basins of the Southern Alps. Sedimentation starts with fluvial conglomerates (Conglomerato Basale) irregularly covering metamorphic rocks, which are the source of the clasts. Thickness changes (from 0 to a few tens of meters) are ascribed to the irregular topography mantled by this unit. The Conglomerato Basale is sharply covered by a complex and lithologically heterogeneous unit known as the Collio Formation. Recently, a lithostratigraphic revision of the nomenclature of this unit has been proposed (AAVV, 2005) in the frame of the project of the new 1:50.000 geological map of Italy (CARG Project). The lithostratigraphic subdivision followed in this paper is that of the 1:50.000 geological sheet "Sondrio" and "Clusone", in which part of the study area is mapped (Carta Geologica d'Italia,

foglio 56 “Sondrio”, in press). After the deposition of the Conglomerato Basale, pyroclastic flows mark the base of the Cabianca Volcanite (Lower Collio Fm. *Auct.*), which is up to 800 meters thick in the depocentre. The Cabianca Volcanite consists of (Cadel et al., 1996): a lower volcanic unit; a middle unit consisting of alternating sediments (sandstones and siltstones) and pyroclastic deposits; and an upper unit consisting mainly of ignimbritic flows. The Cabianca Volcanite pinches out toward the borders of the Permian basin.

The Cabianca Volcanite is covered by clastic sediments of the overlying Pizzo del Diavolo Formation (PDV). This unit consists of continental deposits (Casati and Gnaccolini, 1967; Cadel et al., 1996; Sciunnach, 2001) spanning from coarse conglomerates and time-equivalent, thick sandstone bodies to dark siltstones, locally alternating with microbial carbonates. The top of the PDV is marked by an angular unconformity at the boundary with the Upper Permian alluvial sediments of the Verrucano Lombardo, whose deposition postdates the end of the Early Permian tectonic stage in the Southern Alps. The angular unconformity reflects a tectonic stage which is responsible for the tilting of about 10-20° of the Lower Permian succession before the deposition of the Verrucano Lombardo. The tilting is toward the north, so that the Verricano Lombardo lies in the southern area on older successions. Here it covers directly the Cabianca Volcanite, as the Pizzo del Diavolo Formation was completely eroded before the deposition of the Verrucano Lombardo (Fig. 2, 3).

The Orobic Basin of the Southern Alps is affected by syndepositional extension. Tectonic control is documented by the sharp closure of sedimentary units against highs and rapid facies and thickness changes (Casati and Gnaccolini, 1967; Cadel et al., 1996; Perotti and Siletto, 1996; Cassinis et al., 1997), as well as the identification of paleofaults (Blom and Passchier, 1997; Forcella and Siletto, 2001). The effects of the syndepositional tectonics, recorded by the facies distribution and changes, are documented by seismically-induced sediment deformation and liquefaction, reported for the first time in this basin by Ronchi et al. (2005), in sandy and shaly deposits.

3. - Stratigraphy

The study area (Fig. 2) is part of the Orobic Basin. It is characterized by a thick (more than 1000 m) succession of prevailing continental clastics with intercalations of ignimbritic flows and tuffs (Pizzo del Diavolo Formation, PDV) resting on up to 800 m of prevailing pyroclastic flows of the Cabianca Volcanite. The studied sections belong to the PDV, which can be divided into three parts: Lower, Pelitic and Upper lithozones (Fig. 3). The Lower Lithozone is mainly characterized at the

southern edge of the study area by conglomeratic bodies (clasts derive from Early Permian volcanic rocks; Val Sanguigno Conglomerate of Cadel et al., 1996) which make a transition northward to a massive sandy unit and, more distally, to fine-grained, bedded sandy and silty deposits (Fig. 3). Facies changes indicate a transition from the border of the basin (south, coarser) to a distal part (north, finer). Sedimentological features reflect a proximal fan system (L-PDVc in Fig. 3) where mass-flow phenomena dominate, distal fan-terminal fan settings (L-PDVb in Fig. 3) with prevailing sandy sheet-flow processes in the central area and, more to the north, silty flood-plain environments, where fine-grained sheet-flow events dominate (L-PDVa in Fig. 3). In the northern part of the Lower Lithozone, a silty layer containing calcitic nodules with a chicken-wire texture (interpreted as evidence of sulphate precipitation at the border of an ephemeral lake during arid intervals, later substituted by calcite) can be followed. The Lower Lithozone is characterized by a fining-upward trend which ends with the deposition of the Pelitic Lithozone (P-PDV).

The Pelitic Lithozone (Fig. 2, 3) consists of laterally-continuous siltstones and shales with carbonate nodules and layers of microbial carbonates. This unit (up to 40 m thick) separates the Lower Lithozone of PDV, exclusively clastic, from the Upper Lithozone, consisting of sandstone and siltsone layers alternating with volcanic flows. Carbonates are represented by massive, yellowish continuous beds from a few to 0.3 m thick, with microbial parallel laminations. Carbonates alternate with dark, laminated pelites, often containing carbonate nodules. Pelitic facies are frequently characterized by the presence of tracks of small reptiles and amphibians. This facies association indicates alternating conditions of ephemeral shallow fresh-water basins (deposition of microbial carbonates) with drying of these ponds, as documented by mud-cracks and vertebrate footprints. A slumped interval about 4 m thick is present within the Pelitic Lithozone, about 25-30 m below the top of the unit. This slump can be physically followed throughout the study area (Fig. 2) at the same stratigraphic position within the unit, demonstrating that the deposition of the Pelitic Lithozone was synchronous.

The Upper Lithozone is characterized at the base by thin ash flows (U-PDVa), in beds up to 0.3 m thick. The contact with the underlying Pelitic Lithozone is sharp and can be traced throughout the study area (Fig. 2). The basal volcanic level of the Upper Lithozone, about 10 m thick, gradually evolves to a laterally continuous succession (U-PDVb) of alternating sandstones and volcanic flows (mainly tuff and thin ignimbritic flows). An increase in the occurrence of fine-grained ash layers (U-PDVc) is recorded at the top of U-PDVb. The upper part of the Upper Lithozone consists of fine-graded sandstones and siltstones with intercalations of oncoidal carbonates (U-PDVd). This unit reflects periodic subaqueous conditions, which are necessary to explain the deposition of oncoidal carbonates. Oncoids are up to 0.05 m in size, documenting the existence of high-energy

episodes. The fine-grained siltstones and sandstones associated with the oncoidal carbonates are rich in reptilian and amphibian tracks, documenting that the water depth was reduced and that subaqueous episodes were ephemeral. The Upper Lithozone is characterized by a generally fining-upward trend. The lateral continuity of the facies in the Upper Lithozone suggests an homogeneous evolution, without the proximal to distal trend recognised in the underlying Lower Lithozone (Fig. 3). This more homogeneous depositional setting suggests a widening of the basin during the deposition of the Upper Lithozone. The PDV is unconformably covered by the Late Permian Verrucano Lombardo (Fig. 2).

4 – Description of the deformation structures

The application of an appropriate classification scheme for sediment deformation structures is difficult because they occur in a large variety of complex geometries and morphologies. Moreover, the processes responsible for their genesis can be interpreted in a different way: purely depositional processes versus those induced by seismic shocks.

As suggested by Montenat et al. (2007), we have grouped the observed soft-sediment deformation structures in two main categories: i) ductile deformation structures and ii) brittle structures, which are described and interpreted as follows.

i) Ductile deformation structures

Ball-and-pillow structures

Ball-and-pillow structures are characterized by a more or less periodically arranged suite of deformed, concave upward bodies (pillows) or concentric ball morphologies (balls) made of silt and sand whose original layering (parallel to the basal surface) is folded upwards and is truncated at the top surface (Fig. 4, 5). The sediment both within and surrounding the structures is of similar, fine sand grain-size composition.

These structures are common in fine-grained successions of the Lower Lithozone and their frequency increases up-section, until the deposition of the playa-lake succession of the Pelitic Lithozone. With the volcanic flows and sandstones of the base of the Upper Lithozone these structures almost disappear.

The observed ball-and-pillow structures are usually symmetrical and occur at a horizontal spacing of 0.05 to 0.50 m throughout the beds, forming a series of laterally connected synforms and antiforms up to 0.40 m high. Their cores (typically fine- to medium-grained sand) show concave-

upward laminae that are conformable to the basal shapes. The layered internal structure is lost in the sandy horizon below the pillows. The top surface of the pillow beds is commonly truncated due to erosion, indicating that they were formed close to the depositional surface.
The observed concentric sand balls are rounded structures that have completely lost their continuity with the upper strata and internally display simple, concentric laminae, often with an inner massive core. Individual balls have diameters that range from 0.05 to 0.30 m. This structure is commonly found `floating' within deposits showing irregular convolute stratification.
Similar deformational structures, typically displaying a ball-and-pillow shape, have been described by Pettijohn and Potter (1964), Allen (1986), Moretti et al. (1995), Rossetti, (1999), and Rodrıguez-Pascua et al. (2000).

Plastic intrusions

They are small diapir-like structures made of fine material (argillaceous fine sands and silts) which intrudes and deforms the overlying beds (Fig. 6, 7, 8).
Examples of plastic intrusions have been observed at several levels in the lower part of the studied succession. They are more frequent in the fine-grained sediments of the Pelitic Lithozone.
The observed plastic intrusions usually occur at rather regular intervals across single-layered sand beds, at a horizontal spacing of 0.01–0.30 m and height up to 0.07 m.
In a small number of cases, the top of the intrusion shows veins (sand dykes) of the same material, often oblique and ending upward. Depending on the consistency and homogeneity of the overlying beds, the intrusion may go through one to several centimetres of sedimentary cover. Furthermore, incipient doming of the silts at the contact with the overlying laminites is locally observed.
In a few cases, plastic intrusions reach the surface and the sweeping off of mud and sands produce the classical “sand volcanoes” (cm scale) set out as flattened cones along fissures. In this case the deformation occurs on the exposed surface or in the immediate subsurface. Remnants of the cone are exceptional in the study area: the “volcanoes” generally are eroded and sealed by subsequent undeformed deposits. The core of the volcano shows a fluidal structure due to the extrusion of fluidized sediment.
Comparable deformation structures have been described extensively in the literature (Hempton and Dewey, 1983; Scott and Price, 1988; Alfaro et al., 1997; Rodrıguez-Pascua et al., 2000, Ronchi et al., 2005).

Disturbed lamination

This structure, typically developed in finely laminated sediments (argillaceous fine sands and silts), consists of bundles of laminae that display irregular thinning and thickening without losing their lateral geometric continuity (Fig. 7, 8, 9). Thickness of the disturbed laminae ranges from 0.02 to 0.15 m. In the study area, this type of deformational structure is rather common in laminated sediments of the upper part of the Lower Lithozone. Layers with disturbed laminations are generally perfectly parallel to the bedding of overlying and underlying layers, suggesting that an origin related to sediment injection (i.e. pseudolayers which generally alternate parallel to cross relationships with bedding; Parize and Fries, 2003) is unlikely. In a few cases, laminae are sharply constricted at intervals, giving a morphology of loops or links of a chain (loop bedding). The thickness of the loop bedded layers ranges typically from 0.005 to 0.025 m and the loops end laterally at centimetric intervals. Disturbed lamination within the laminites is frequently associated with the presence of micro-faults

Comparable deformational structures, typically displaying disturbed lamination (and loop bedding), have been described by Cole and Picard (1975), Gibling et al. (1985), Allen (1986), Calvo et al. (1998), Rossetti, (1999), Rodrıguez-Pascua et al. (2000), Ronchi et al. (2005), Montenat et al. (2007) and Moretti and Sabato (2007).

Irregular convolute (or highly distorted) stratification and fractured layers

This type of structure refers to beds that show folded layers with irregular morphologies and sizes or highly distorted stratification, with fragment-supported and matrix-supported textures between undeformed beds (Fig. 5). Locally, a transition from undisturbed laminites to folded and fractured layers ending with a clastic-textured sediment has been observed. Fragments made of single and/or sets of laminites are several millimetres long and are commonly found `floating' within these highly distorted deposits. The thickness of these beds ranges from 0.10 to 2.00 m. The top of the convolute stratification is generally sharply overlain by horizontally laminated sediment or completely homogeneous, massive beds. This convolute stratification occurs in silty to fine-grained sandstones and is associated typically with playa-lake sediments (Pelitic Lithozone).

Similar deformational structures, typically displaying an irregular convolute stratification, have been described by Pettijohn and Potter (1964), Allen (1986), Rossetti, (1999), and Rodrıguez-Pascua et al. (2000), Ronchi et al. (2005), Montenat et al. (2007).

Recumbently-folded laminations

This structure consists of cross-sets with overturned internal stratification (slumps) at different scales (from cm to m), which form recumbent folds with either horizontal or slightly inclined axial planes. They are commonly observed in lacustrine deposits which display regular and delicate varved lamination (Sims, 1975; Hempton and Dewey, 1983; El-Isa and Mustafa, 1986; Ringrose, 1989; Beck et al., 1992; Moretti and Sabato, 2007).

Two major deformed beds (up to 4.0 m thick) showing complex folding have been observed in the study basin. In these two beds the dominant deformation structures are represented by recumbently-folded laminations at different scales, which are associated with other types of structures.

The first bed (Fig. 10) consists of a layer about 1.5 m thick of parallel-laminated siltstones and shales, deformed by isoclinal recumbent folds, commonly associated with pillow-like structures and irregular convolute stratification. The bed is characterized at the top by the presence of mud cracks which indicate, in agreement with the fine-grained size of the sediments, deposition on a very low-angle slope, along which, due to the liquefaction, the sediments slid. The slumped layer pinches out in a few hundreds of meters. Both the base and the top are sharp, supporting the existence of a basal detachment surface probably driven by the different compaction/cohesion of the underlying beds.

The second very thick deformed bed (Fig. 11) developed in an alternation of dark shales and carbonate layers (Pelitic Lithozone PDF). This deformed horizon, about 4 m thick, can be followed for at least 5 km. The folds (especially at the small scale) affect both the carbonates and pelitic layers, are disharmonic and show evidence of subsequent flattening. The top is sharp and covered by lithofacies identical to those of the deformed beds.

Asymmetrical deformations are observed also in plastic intrusions (i.e. Fig. 6), suggesting that deposition and deformation occurred on low-angle slopes. The lateral evolution of the depositional environment (from alluvial fans to playa lakes) points to the existence of low-angle slopes. Field et al. (1982) demonstrate that seismic shocks are able to trigger slumps in water-saturated sediments on slopes less than 1° steep and it is likely that similar angles were present in the studied basin. Furthermore, earthquakes could have produced tilting of part of the basin and/or gentle bulges, creating local conditions favourable to the development of slumps.

ii) Principally brittle structures

Sand dykes (Fig. 4, 6, 7, 9, 12)

This structure consists typically of sand-filled fractures, commonly rooted in a structureless sand bed (sediment source) and cutting confining horizons of distinct lithologies. Sand dykes are steeply inclined to vertical paths, up to a few centimetres in length (usually <0.20 m) and less than 0.05 m in diameter, which cut sharply through the deformed beds. In the study area these structures are generally isolated and locally form bifurcated paths (Fig. 9). Due to the type of exposure, dykes have been observed in vertical section so that it was not possible to confidently measure their orientation. Dykes are straight to sinuous in vertical view. Sinuosity of the dykes is enhanced by post-depositional compaction after the emplacement of the dykes, with the development of ptygmatic folds (Laubach et al., 2000). The dyke fills consist of homogeneous medium- to very fine-grained sand of the same nature as the beds from which the dykes project upward or downward.

A network of dykes, often connected, formed of major sand intrusions is commonly observed. Deformed lamination (concave upward) is common at the top of the dykes (Fig. 6). Dykes locally show cross-cutting relationships with ductile deformation structures (Fig. 6). The co-occurrence of ductile (older) and brittle (younger) deformations suggests that the sediments experienced a ductile deformation when they were still plastic, whereas once they became more cohesive they were affected by brittle deformation. In some cases it is possible to observe plastic deformations partially eroded before the deposition of overlying layers. The same sediments were thus affected by two successive seismic deformations, at a different degree of induration/compaction.

Two categories of dykes are present in our case study: injection (or intrusion) dykes (Fig. 6) and neptunian dykes (Fig. 7, 9). Intrusion dykes are formed by injection of sediment from some underlying source and emplaced upwards under abnormal pressure. These dykes show typical dish and pillar structures and other features related to fluid escape and sweeping of the conduits (wrenching out of fragments of the walls). Neptunian dykes are formed by introduction of material from above, either under pressure or by simple filling of pre-existing cracks or fissures.

Similar deformational structures have been described extensively in the literature (e.g. Allen, 1986; Calvo et al., 1998; Rossetti, 1999; Rodrıguez-Pascua et al., 2000; Ronchi et al., 2005; Montenat et al., 2007; Moretti and Sabato, 2007).

Autoclastic breccias

Autoclastic breccias (Fig. 12) result from the brecciation of indurated deposits, commonly represented by cohesive silty and fine-grained sand beds. The fragments of the original sediment (often polygonal and variable in size, from 0.01 to 0.2 m) generally show a good fit with their neighbours, from which they are separated by fluidized material intruding between the fragments. In some cases, large elongated fragments `float' within the sediment.

The brecciation planes are vertical to subvertical, extremely ragged with small sharp peaks. Autoclastic breccias are locally associated with deposits showing pillow-like structures and irregular convolute stratification, indicating that the same sediment suffered both ductile deformation (convolute stratification) and brittle deformation (autoclastic breccias). The association of breccias (from indurated deposits) and plastic sediments can be explained: 1) by a change in time of the degree of cohesion of the different layers of the deposits, which suffered at least two different deformation stages; or 2) by the different physical condition of the layers of the sediment (different cohesion/permeability related to different grain size and thus different reaction to the same stress). Actually, autoclastic breccias mainly derive from finer (and thus more cohesive) sediments, whereas the ductile deformation is mainly accommodated by slightly coarser, water-saturated (at the moment of deformation) sands, thus supporting the second hypothesis. The possibility that these authoclastic breccias could be generated by disruption by volcanic gases venting through the sediments (tuffisite of Cloos, 1941) is excluded, as the stratigraphic setting of the studied area indicates that the volcanic centres were relatively distant (i.e. absence of lava flows and volcanic dykes throughout the study area) and because the breccia layers are generally horizontal and do not follow vertical paths (as should be expected in case of flowing gases).

5 – Discussion

5.1 - Mechanism of deformation

Different possible explanations may account for the genesis of the observed soft-sediment deformation structures. Field evidence shows that deformation formed in loose, unconsolidated to semi-consolidated fine-grained, water-saturated muddy and sandy deposits and was induced chiefly by liquefaction and/or fluidization processes, producing a variety of deformation structures (Lowe, 1975; Allen, 1982; Owen, 1987). Liquefaction processes reduce the shear strength and promote the gravitational collapse of higher density layers and the rise of less dense layers. Liquefaction is a

temporary loss of strength caused by the breakdown of the grain framework and the transfer of grain support to the pore fluid (Lowe, 1975; Allen, 1982; Owen, 1987). This process has been assumed to play a role in generating soft-sediment deformation structures (Lowe, 1975; Allen and Banks, 1972; Leeder, 1987; Tsuji and Miyata, 1987; Owen, 1996) and could be related to several natural trigger mechanisms. The interpretation of the actual origin of deformation structures observed in the field can often be difficult. In particular, to infer a probable seismic origin (Ishihara, 1993; Obermeier, 1996a; 1996b; Obermaier et al., 2001; Montenat et al., 2007; Moretti and Sabato, 2007), it is necessary to exclude the influence of other processes.

Ball-and-pillow, plastic intrusions and irregular convolute (or highly distorted) stratification have been commonly interpreted (Allen, 1982; Mills,1983) as related to rapid sand accumulation onto water-saturated muds (Potter and Pettijohn, 1977). These ductile deformation structures are also related to seismic shocks on water-saturated sediments (Montenat et al., 1987; Cojan and Thiry, 1992; Guiraud and Plaziat, 1993). In this case, the formation of ball-and-pillow, plastic intrusions and irregular convolute (or highly distorted) stratification was initiated by liquefaction, caused by seismic shocks, of some definite layers within packages of layered sands or silt that were forced to fold as a result of the upward flow of liquefied sediment. More chaotic deformation occurred in less compacted areas with more liquefied, less viscous sediments, resulting preferentially in irregular, convolute folds. The correct interpretation of the origin (seismic versus sedimentary load) of these structures is challenging (Moretti and Sabato, 2007). In the observed structures, evidence of rapid load of sediments as a cause of liquefaction is unlikely, as the dominant sedimentation processes are related to traction currents with deposition of relatively thin layers of sediment for each depositional event. Furthermore, deformed structures are frequently eroded at the top (i.e. Fig. 4 and Fig. 6b), indicating that the formation of these structures occurred before the deposition of the overlying layers. Therefore, the observed ball-and-pillow structures, plastic intrusions and irregular convolute stratification can be confidently ascribed to a seismic shock, rather than to load effects.

Sand dykes, commonly observed in the study area, have been widely interpreted to represent flow paths with fluidized sediments being injected from surrounding strata as a result of increasing interstitial pore pressure (e.g. Daley, 1971). The origin of injection dykes is ultimately related to liquefaction of a basal saturated sand (or silt) bed, possibly triggered by seismic shocks (Audemard and De Santis, 1991), whereas neptunian dykes result from extension (Moretti and Sabato, 2007).

Thinning and thickening of the laminae (disturbed lamination) reflect a ductile–brittle behaviour of the sediment as supported by the development of normal micro-faulting (i.e. fig. 6d).

Autoclastic breccias record brittle deformation which occurred shortly after deposition. Sesimic shocks produced ductile deformation in non-cohesive, water-saturated sediments, whereas brittle

structures were formed in more cohesive sediments. The occurrence of both ductile and brittle deformation in the same layer (Fig. 6c) indicates that seismic shocks caused different effects according to the state of the sediment.

The observed association of deformed structures is confidently explained by seismic activity, in basins which were bordered by strike-slip faults, active during the deposition of the Lower Permian succession (Tab. 1). Earthquakes associated with dislocation along the border faults of the basin explain most of the observed deformations in unconsolidated to semi-consolidated sediments, as suggested by the following lines of evidence:

- Deformation structures developed during the deposition of specific stratigraphic intervals, separated by similar but undeformed sediments. The studied deposits show a recurrence of seismic events in time, as recorded by successive beds with soft-sediment deformation, separated by undeformed deposits. This behaviour is typical of seismically active areas. Studies in modern environments suggest that activity on a single strike-slip fault may produce major earthquakes within short time periods, that range from hours to weeks or decades to millenia (e.g. Crone et al., 1997).
- The basin floor was flat to very gently sloping, so there is no evidence for substantial slope failure that could account for all the soft-sediment deformation of the study area. Nevertheless, the vergence of some ductile deformation structures (Fig. 6) and the presence of the slump layers (Fig. 10 and 11) indicate the existence of low-angle slopes. Slump folds triggered by earthquakes are documented on slopes even of 0.25° (Field et al., 1982) and have been observed also in the depocentral area of lakes (Moretti and Sabato, 2007), confirming that slump generation does not require steep slopes.
- A slump layer (the one within the Pelitic Lithozone) can be correlated over distances up to several kilometres within the study area, supporting a major seismic event. The presence of tetrapod footprints and mud cracks immediately above and below the slump are compatible with the existence of a very low angle of the depositional surface.
- Sedimentary structures indicate that rapid accumulation of sediment did not occur in the studied succession, precluding the origin of the thixotropic failure of the clays due to overloading.
- The deformed structures observed in the PDV occur within a seismically active basin (i.e. Cadel et al., 1996), with deposition close to a major fault zone that remained active throughout Lower Permian.

Determining the magnitudes of the earthquakes that induced the formation of the soft-sediment deformation structures in the study area is difficult. Different methods have been developed to define the intensity of an earthquake (Obermeier et al., 2001 and references therein): a) the magnitude bound method, which considers the distance of paleoliquefaction features; b) the cyclic stress method (Seed et al., 1985); c) energy-based solutions; d) the Ishihara method, which uses dyke height. These approaches are generally used to determine the intensities of Holocene earthquakes affecting unconsolidated deposits, whereas they are not easily applied to lithified and deformed successions, where magnitude can be only roughly evaluated.

The interpretation of seismites in terms of the magnitudes of the seismic shocks has generated a considerable literature (Sims, 1975; Hempton and Dewey, 1983; Allen, 1986; Audemard and De Santis, 1991; Cojan and Thiry, 1992; Guiraud and Plaziat, 1993; Obermaier, 1996a, 1996b). Many authors (Youd, 1977; Allen, 1986; Scott and Price, 1988; Audemard and De Santis, 1991; Galli, 2000) consider Richter magnitude > 5 as the lowest magnitude that can produce significant liquefaction in near-surface, water-saturated, semi-consolidated to unconsolidated sediments, because earthquakes of lower magnitude are not generally of sufficient duration to cause liquefaction. Beside earthquake intensity, distance from the foci of the earthquakes is important (historical data show that 79% of liquefaction occurs within 30 km from the depocentre; Galli, 2000), as liquefaction phenomena decrease with distance from the earthquake following empirical equations (Galli, 2000). Shocks of higher intensity (magnitudes >6) are required in order to produce liquefaction at distances greater than 15±20 km from the epicentre (e.g. Sims, 1975; Moretti et al., 1995; Mohindra and Bagati, 1996; Moretti and Tropeano, 1996; Blanc et al., 1998; Galli, 2000). Sand dykes occurring in lacustrine and fluvial deposits have been interpreted as related to earthquakes of magnitudes ranging from 5 to 8 (Audemard and De Santis, 1991; Obermeier et al., 1993). A rather similar rank of earthquake magnitudes (5.5–8) has been deduced for ball-and-pillow structures developed in littoral marine, deltaic or fluvial deposits (Cojan and Thiry, 1992; Guiraud and Plaziat, 1993; Obermeier, 1996a). Besides these general determinations of the possible magnitude of an earthquake, interpretation of paleo-magnitude heavily relies upon the local tectonic/stratigraphic setting. A shallow (less than 50 km) hypocentral depth can cause more severe shaking close to the epicentral area than a deeper earthquake and thus more liquefaction structures. Away from the epicentre, however, shaking may be less severe for a shallower earthquake than for a deeper one (Obermeier, 1996b) so that deeper earthquakes can generate liquefaction at greater distance from the epicentre than shallower earthquakes (fig. 42 in Obermeier, et al., 1996b)

The observed high density of seismically induced structures (both in space and time) indicates that the study area was close to the active faults that bordered the extensional basin (and thus to the

hypocentres of the earthquakes, which were located in the crust) and that seismic activity was frequent. The recording of liquefaction requires sediment in a saturated state and it is realistic to suggest that the observed succession was not always in this state. It follows that only earthquakes of sufficient magnitude affecting liquefaction-prone sediments are recorded by seismites. Based on this literature, Richter earthquake magnitudes of 5 or greater would have repeatedly affected deposition in the study area and produced widespread sediment failure, folding and liquefaction in unconsolidated or semi-consolidated deposits. Soft-sediment deformation structures that we interpret as seismites have been ordered according to a rank of the possible earthquake magnitudes (Tab. 1). The relationship between magnitude and type/size of deformation is controlled by a number of factors in addition to the magnitude of the earthquake and distance from the epicentre, such as saturation state, grain size of the sediments (which controls the drainage), duration of the seismic shocks, depth of the hypocentre, slope angle and amplification phenomena. The stratigraphy and architecture of the basin played a major role in the amplification of bedrock accelerations. The PDV, consisting of loose, water-saturated sediments, rests on up to 800 m of ignimbritic flows (CAB) which cover the Variscan metamorphic rocks. The differences in the physical properties of the multilayer favoured the reflection of the waves, increasing the effects of the seismic shocks at least in terms of duration and shaking (Obermeier, 1996b), a fact that highly increases the potential for triggering liquefaction of the sediments.

Nevertheless, the studied sediments show similar features and textures, were deposited in the same depositional system and are placed relatively close to the fault-controlled basin borders. These homogeneous conditions support the hypothesis that the size and type of seismites may be a proxy for the relative intensity of the seismic shocks, so that, in the same basin and with similar lithologies, we suggest that larger structures (i.e. slump in the Pelitic Lithozone) likely indicate higher magnitude earthquakes.

5.2 - Stratigraphic distribution of seismites

The stratigraphic evolution of the Lower Permian succession of the Orobic Basin reflects a strong tectonic control on sedimentation at different scales. Facies and thickness changes and volcanic activity have been recognized as proof of tectonic control on basin evolution since the oldest studies on the Orobic Basin (i.e. De Sitter and De Sitter-Koomans, 1949). Syndepositional tectonics is also documented by the abundance, stratigraphic distribution and nature (in terms of type of deformation, size and frequency) of soft-sediment deformation structures. The nature and abundance of deformation structures are controlled by the type of sediment, but the distribution of

seismically induced structures is not homogeneous in similar lithologies across the studied sections, emphasising that not only lithology, but also the stratigraphic evolution of the basin, controls the presence and nature of seismites. This observation suggests that seismic activity was not constant during the deposition of the Lower Permian succession of the Orobic Basin, but it was more intense at specific stratigraphic intervals. The vertical arrangement of the succession reflects two different moments of the basin evolution, separated by a fine-grained interval (Pelitic Lithozone). The transition form an articulated setting (Lower Lithozone) to an homogeneous sedimentation of pelitic playa-lake deposits reflects an important and rapid change in the basin architecture, which was followed by a sharp reprise of the volcanic activity (base of the Upper Lithozone). Nevertheless, the highest concentration of seismites is observed in the fine facies (L-PDVa) of the upper part of the Lower Lithozone and especially in the Pelitic Lithozone (P-PDV), suggesting that the initiation of the playa-lake environment was favoured by a major tectonic pulse able to drive the basin evolution. The nature of the sediments, the homogeneous facies association (siltstones and shales alternating with microbial carbonates) and the presence of abundant mud-cracks point to the development of an almost flat basin floor above a previous fan system with different facies associations.

The onset of this playa-lake setting is also coupled with the most impressive evidence of seismic activity in the studied succession, represented by the metre-thick slump layer in the upper part of the Pelitic Lithozone. The stratigraphic position of the large slump overfold immediately predates the return of volcanic activity which characterizes the base of the Upper Lithozone and could confidently be associated with an acme of the seismic activity. The slumped layer in the Pelitic Lithozone probably also reflects the most intense earthquake recorded in the studied succession.

6 – Conclusions

The sedimentological analyses of the Lower Permian succession of the Orobic Basin (Southern Alps) allowed us to identify different types of soft-sediment and liquefaction structures which document the effect of seismic shocks on water-saturated sediments deposited on low-angle slopes or on a flat basin floor. Both the sedimentological features and the geological context of the basin confidently support the interpretation of a seismic origin for these structures. Seismic structures differ both in size (from centimetric to plurimetric) and in the physical properties of the involved sediments.

Seismites are mainly developed in fine-grained sediments. Alternations of fine to medium sands with pelites is the most common sedimentary setting in which they develop. The largest seismic structure is represented by a metre-thick slumped interval of alternating microbial carbonates and dark pelites, which can be followed for at least 5 km. The slump affects a playa-lake succession and developed on a very low-angle slope.

The distribution and frequency of seismites is not constant in these fine-grained sediments, suggesting a discontinuous tectonic activity. The analysis of the stratigraphic distribution of the seismic structures indicates that their highest concentration coincides with major changes in the stratigraphic architecture of the basin: at the top of the Lower Lithozone and immediately before the volcanic activity documented at the base of the Upper Lithozone. This distribution reflects the relationships between syndepositional tectonics (i.e. intensity and frequency of earthquakes recorded by seismites) and major stratigraphic changes, in terms of both basin architecture and volcanic events.

The generation of the described seismites requires the magnitude of the earthquakes which affected the studied basins to have been largely higher than 5. Considering the thickness, distribution and environmental setting of the slump in the Pelitic Lithozone, we realistically suggest that the magnitude probably reached also values of 7 or higher. Considering the nature of the Orobic Basin, the magnitude documented by the described seismites was likely close to the real magnitude of the earthquakes, as the position of the epicentres was likely placed within the basin itself or at its fault-controlled borders. The effects of seismic waves were amplified due to the stratigraphic setting of the Orobic Basin. The deposition of loose continental sediments (PDV) directly above a thick volcanic wedge (CAB) overlying a metamorphic basement with higher density greatly enhanced the effects of the seismic waves, at least in terms of the duration of seismic shaking, favouring the diffuse development of seismites.

Acknowledgments

M. Fonnesu, D. Paramatti, R. Pessina, V. Rossi and A. Tessarollo are warmly acknowledged for their support during field work. This work benefitted from the careful and invaluable comments from two anonymous reviewers and from the guest editors of the volume (G. Owen and M. Moretti) on the first version of the manuscript. Their suggestions are here warmly thanked, as well as the fruitful discussion with R. de Franco (CNR-IDPA, Milan) on the amplification of seismic shocks.

References

AAVV, 2005. Riunione Gruppo di Lavoro sulle Coperture Sedimentarie – Comitato d'area per le Alpi centrali, orientali ed occidentali. Apat, http://www.apat.gov.it/site/_files/SuoloCARG/verbale11.pdf

Alfaro, P., Moretti, M., Soria, J.M., 1997. Soft-sediment deformation structures induced by earthquakes (seismites) in the Pliocene lacustrine deposits (Guadix-Baza Basin, Central Betic Cordillera). Eclog. Geol. Helvet. 90, 531–540.

Allen, J.R.L., 1982. Sedimentary Structures. Their Character and Physical Basis. Elsevier, Amsterdam.

Allen, J.R.L., 1986. Earthquake magnitude-frequency, epicentral distance, and soft-sediment deformation in sedimentary basins. Sediment. Geol. 46, 67–75.

Allen, J.R.L., Banks, N.L., 1972. An interpretation and analysis of recumbent-folded deformed cross-bedding. Sedimentology 19, 257-283.

Arthaud, F., Matte, P., 1977: Late Paleozoic strike-slip faulting in southern Europe and northern Africa: Result of a right-lateral shear zone between the Appalachian and the Urals – Geological Society of America Bulletin 88, 1305-1320.

Atkinson, G., 1984. Simple computation of liquefaction probability for seismic hazard applications. Earthquake Spectra 1, 107–123.

Audemard, F.A., De Santis, F., 1991. Survey of liquefaction structures induced by recent moderate earthquakes. Bull. Int. Assoc. Engin. Geol. 44, 5–16.

Beck, C., Rochette, P., Tardy, M., 1992. Interprétation en termes de paléoséismicité de niveaux déstructurés intercalés dans des rythmites lacustres quaternaires des Alpes Nord-Occidentales. C. R. Acad. Sci. 315, 1525–1532.

Blanc, E.J.-P., Blanc-Alétru, M.-C., Mojon, P.-O. 1998. Soft-sediment deformation structures interpreted as seismites in the uppermost Aptian to lowermost Albian transgressive deposits of the Chihuahua basin (Mexico). Geol. Rundsh.86, 875-883.

Blom, J.C., Passchier, C. W., 1997. Structures along the Orobic thrust, Central Orobic Alps, Italy – Geol. Rundsh. 86, 627-636.

Cadel, G., Cosi, M., Pennacchioni, G., Spalla, M.I., 1996. A new map of the Permo-Carboniferous cover and Varisican matamorphic basament in the Central Orobic Alps, Southern Alps-Italy: structural and stratigraphical data - Mem.Sci.Geol. 48, 1-53.

Calvo, J.P., Rodriguez-Pascua, M.A., Martin-Velazquez, S., Jimenez, S., De Vicente, G., 1998. Microdeformation of lacustrine laminite sequences from Late Miocene formations of SE Spain: an interpretation of loop bedding. Sedimentology 45, 279–292.

Carta Geologica d'Italia 1:50.000, foglio 56 "Sondrio", in press. http://www.apat.gov.it/Media/carg/Allestimento/056_Sondrio/056.htm

Casati, P., Gnaccolini, M., 1967. Geologia delle Alpi Orobie Occidentali. Riv. Ital. Paleont. 73, 25-162.

Cassinis, G., Massari, F., Neri, C., Venturini, C., 1988, The continental Permian in the Southern Alps (Italy). A review. Zeitschrift Geologische Wissenschaften 16, 1117-1126.

Cassinis, G., Perotti, C.R., Venturini, C., 1997. Examples of late Hercynian transtensional tectonics in the Southern Alps (Italy). In: Dickins JM (ed) Late Paleozoic and early Mesozoic Circum-Pacific events and their global correlation, vol 10. Cambridge University Press, World and Regional Geology, 41–49

Cloos H., 1941. Bau und tatigkeit von tuffschloten, Geologische Rundschau 32, 705–800.

Cojan, I., Thiry, M., 1992. Seismically induced deformation structures in Oligocene shallow-marine and eolian coastal sands (Paris Basin). Tectonophysics 206, 79–89.

Cole, R.D., Picard, M.D., 1975. Primary and secondary structures in oil shale and other fine grained rocks, Green River Formation (Eocene), Utah and Colorado, Utah. Geology 2, 49–67.

Crone, A.J., Machette, M.N., Bowman, J.R., 1997. Episodic nature of earthquake activity in stable continental regions revealed by palaeoseismicity studies of Australian and North American Quaternary faults. Aust. J. Earth Sci. 44, 203-214.

Daley, B., 1971. Diapiric and other deformational structures in a Oligocene argillaceous limestone. Sedim. Geol. 6, 29-51.

De Sitter, L.U., De Sitter-Koomans, C.M., 1949. Geology of the Bergamasc Alps, Lombardy, Italy, Leidse Geologische Mededelingen-Leidse 14, 1–257.

Doglioni, C., 1995. Geological remarks on the relationships between extension and convergent geodynamic settings. Tectonophysics 252, 253-267.

El-Isa, Z.H., Mustafa, H., 1986. Earthquake-deformations in the Lisan deposits and seismotectonic implication. Geophys. J. R. Astron. Soc. 86, 413–424.

Field, M.E., Gardner,V., Jennings,A.E., Edwards, B.D., 1982. Earthquake induced sediment failures on a 0.25° slope, Klamath River delta, California. Geology 10, 542–546

Forcella, F., Siletto, G.B., 2001. Structure and stratigraphy of the Permo-Carboniferous cover and variscan metamorphic basement in the northern Serio Valley (Orobic Alps, Southern Alps – Italy): recognition of Permian Faults. Proceed. 2nd Continental Permian Congress, Sept. 1999, Brescia. Monograf. di “Natura Bresciana” 25, 59-64.

Gand, G., Durand, M., 2006. Tetrapod footprint ichno-associations from French Permian basins. In: Non-Marine Permian Biostratigraphy and Biochronology (Ed. by S.G. Lucas and J.W. Schneider), Geological Society, Sp. Publ., 265, 157–177.

Galli, P., 2000. New empirical relationships between magnitude and distance for liquefaction. Tectonophysics 324 (2000) 169–187

Gibling, M.R., Tantisukrit, C., Uttamo, W., Thanasuthipitak, T., Haraluk, M., 1985. Oil shale sedimentology and geochemistry in Cenozoic Mae Sot Basin, Thailand. Am. Assoc. Petr. Geol. Bull. 69, 767–780.

Guiraud, M., Plaziat, J.C., 1993. Seismites in the fluviatile Bima sandstones: identification of paleoseisms and discussion of their magnitudes in a Cretaceous synsedimentary strike-slip basin (Upper Benue, Nigeria). Tectonophysics, 225, 493–522.

Hempton, M.R., Dewey, J.S., 1983. Earthquake-induced deformational structures in young lacustrine sediments, East Anatolian Fault, southeast Turkey. Tectonophysics 98, 7-14.

Ishihara, K., 1993. Liquefaction and flow failure during earthquakes. Geotechnique 43, 351-415.

Laubach, S.E., Schultz-Ela, D.D., Tyler, R., 2000. Differential compaction of interbedded sandstone and coal. In: Forced Folds and Fractures (Ed. by J.W. Cosgrove and M.S. Ameen), Spec. Publ. geol. Soc. London 169, 51-60

Leeder, M.R., 1987. Sediment deformation structures and the palaeotectonic analysis of sedimentary basins, with a case-study from the Carboniferous of northern England. In: Deformation of Sediments and Sedimentary Rocks (Ed. by M. E. Jones and R. M. F. Preston), Spec. Publ. geol. Soc. London 29, 137-146.

Lowe, D.R., 1975. Water escape structures in coarse-grained sediments. Sedimentology 22, 157-204.

Malaveille, J., Guihot, P., Lardeaux, J.M., Gardien, V., 1990. Collapse of thickened crust in the French Massif:Mont Pilat extensional shear zone and St. Etienne Late Carboniferous basin.Tectonophysics 177, 136-149.

Mills, P.C., 1983. Genesis and diagnostic value of soft-sediment deformation structures – a review. Sedim. Geol. 35, 83-104.

Mohindra, R., Bagati, T.N., 1996. Seismically induced soft-sediment structures (seismites) around Sumdo in the lower Spiti valley (Tethys Himalaya). Sedim. Geol. 101, 69-83.

Montenat, C., Barrier, P., Philippe, Ott d′Estevou P., Hibsch, C., 2007. Seismites: An attempt at critical analysis and classification. Sedim. Geol. 196, 5–30

Montenat, C., Ott D'Estevou, P., Masse, P., 1987. Tectonic–sedimentary characters of the Betic Neogene basins evolving in a crustal transcurrent shear zone (SE Spain). Bull. Centres Rech. Explor.-Prod. Elf-Aquitaine 11, 1–22.

Moretti, M., Sabato, L., 2007. Recognition of trigger mechanisms for soft-sediment deformation in the Pleistocene lacustrine deposits of the Sant'Arcangelo Basin (Southern Italy): Seismic shock vs. overloading. Sedimentary Geology 196, 31–45.

Moretti, M., Pieri, P., Tropeano, M., Walsh, N., 1995. Tyrrhenian seismites in Bari area (Murge-Apulian foreland). Atti Convegno `Terremoti in Italia' - Previsione e prevenzione dei danni-Accademia Nazionale dei Lincei 211-216.

Moretti, M., Tropeano, M., 1996. Strutture sedimentarie deformative (sismiti) nei depositi Tirreniani di Bari. Mem. Soc. Geol. It. 51, 485-500.

Obermeier, S.F., 1996a. Using Liquefaction-Induced Featres for Paleoseismic Analysis. In: McCalpin, J.P. (Ed.). Paleoseismology, Academic Press, San Diego 331- 396.

Obermeier, S.F., 1996b. Use of liquefaction-induced features for paleoseismic analysis. An overview of how seismic liquefaction features can be distinguished from other features and how their regional distribution and properties of source sediment can be used to infer the location and strength of Holocene paleo-earthquakes. Engineering Geology 44, 1-76.

Obermaier, S.F., Martin, J.R., Frankel, A.D., Youd, T.L., Munson, P.J., Munson, C.A., Pond, E.C., 1993. Liquefaction evidence for one or more strong Holocene earthquakes in the Wabash Valley of southern Indiana and Illinois, with a preliminary estimate of magnitude. US Geol. Surv. Prof. Paper 1536, 27pp.

Obermaier, S.F., Pond, E.C., Olson, S.M. 2001. Paleoliquefaction studies in continental settings: geologic and geotechnical factors in interpretations and back-analysis. US GEOLOGICAL SURVEY OPEN-FILE REPORT 01-29; on www at http://pubs.usgs.gov/openfile/of01-029.

Owen, G., 1987. Deformation processes in unconsolidated sands. In: Deformation of Sediments and Sedimentary Rocks (Ed. by M.E. Jones and R.F. Preston), Spec. Publ. Geol. Soc. London 29, 11–24.

Owen, G., 1996. Experimental soft-sediment deformation: structures formed by the liquefaction of unconsolidated sands and some ancient examples. Sedimentology 43, 279 294.

Parize, O., Fries, G., 2003. The Vocontian clastic dykes and sills; a geometric model. In: Subsurface sediment mobilization (Ed. by P. Van Resenbergen, A.J. Hillis and C.K. Morley), Geological Society Special Publications, 216, 51-72.

Peressini, G., Quick J. E., Sinigoi, S., Hofmann, A.W., Fanning, M., 2007. Duration of a Large Mafic Intrusion and Heat Transfer in the Lower Crust: a SHRIMP U-Pb Zircon Study in the Ivrea-Verbano Zone (Western Alps, Italy). Journal of Petrology 48, 1185-1218.

Perotti, C.R., Siletto, G.B., 1996. Le caratteristiche geometriche dei bacini permiani tra la Val Camonica e la Val Giudicarie (Sudalpino Centrale). Atti Tic. Sc. Terra 4, 77-86.

Pettijohn, F.J., Potter, P.E., 1964. Atlas and Glossary of Primary Sedimentary Structures. Springer-Verlag, Berlin.

Potter, P.E., Pettijohn, F.J., 1977. Paleocurrents and Basin Analysis. Springer-Verlag, New York.

Ringrose, P.S., 1989. Palaeoseismic (?) liquefaction event in late Quaternary lake sediment at Glen Roy, Scotland. Terra Nova 1 57–62.

Rodríguez-Pascua, M.A., Calvo, J.P., De Vicente, G., Gómez-Gras, D., 2000. Soft-sediment deformation structures interpreted as seismites in lacustrine sediments of the Prebetic Zone, SE Spain, and their potential use as indicators of earthquake magnitudes during the Late Miocene. Sedimentary Geology 135, 117–135.

Ronchi, A., Santi, G., Confortini, F., 2005. Biostratigraphy and Facies of the Lower Permian sedimentary deposits in the Trabuchello-Cabianca Anticline (Orobic Basin, Southern Alps, Italy). In: Lucas, S. G., Ziegler, K E. (eds), The Nonmarine Permian, New Mexico Museum of Natural History and Sciences Bull. 30, 273-281.

Rossetti, D., 1999. Soft-sediment deformation structures in late Albian to Cenomanian deposits, São Luís Basin, northern Brazil: evidence for palaeoseismicity. Sedimentology 46, 1065-1081

Schaltegger, U., Brack, P., 2007. Crustal-scale magmatic systems during intracontinental strike-slip tectonics: U, Pb and Hf isotopic constraints from Permain magmatic rocks of the Southern Alps – Int. J. Earth Sci. (Geol Rundsh) 96, 1131-1151.

Sciunnach, D., 2001. The Lower Permian in the Orobic Anticline (Southern Alps, Lombardy): a review based on new stratigraphic data. Rivista Italiana di Paleontologia e Stratigrafia 101, 47-68.

Scott, B., Price, S., 1988. Earthquake-induced structures in young sediments. Tectonophysics 147, 165–170.

Seed, H.B., Tokimatsu, K., Harder, L.F., Chung. R.L., 1985. Influence of SPT procedures in soil liquefaction resistance evaluations: Journal of Geotechnical Engineering, American Society of Civil Engineers 111, 1425-1445.

Siletto, G.B., Spalla, M.I., Tunesi, A., Lardeaux, J.M.. Colombo, A., 1993. Pre-Alpine structural and metamorphic histories in the Orobic Southern Alps, Italy. In: Pre-Mesozoic Geology in the Alps (Ed. by J.F.Von Raumer and F. Neubauer), 585-598. Springer-Verlag, Heidelberg.

Sims, J.D., 1975. Determining earthquake recurrence intervals from deformational structures in young lacustrine sediments. Tectonophysics 29, 141–152.

Tsuji, T. and Miyata, Y., 1987. Fluidization and liquefaction of sand beds - experimental study and examples from Nichinan Group. J. geol. Soc. Japan 93, 791-808.

Virgili, G., Cassinis, G., Broutin, J., 2006. Permian to Triassic sequences from selected areas of southwestern Europe. In: Non-Marine Permian Biostratigraphy and Biochronology (Ed. by S.G. Lucas and J.W. Schneider), Geological Society, Sp. Publ., 265, 231-259.

Winterer, E.L, Bosellini, A., 1981. Subsidence and sedimentation on Jurassic passive continental margin, Southern Alps, Italy. Bull. Am. Assoc. Petrol. Geol. 65, 394-421.

Youd, T.L., 1977. Discussion of 'Brief review of liquefaction during earthquakes in Japan' by E. Kuribayashi and T. Taatsuoka. Soils Foundation 17, 82-85.

FIGURES

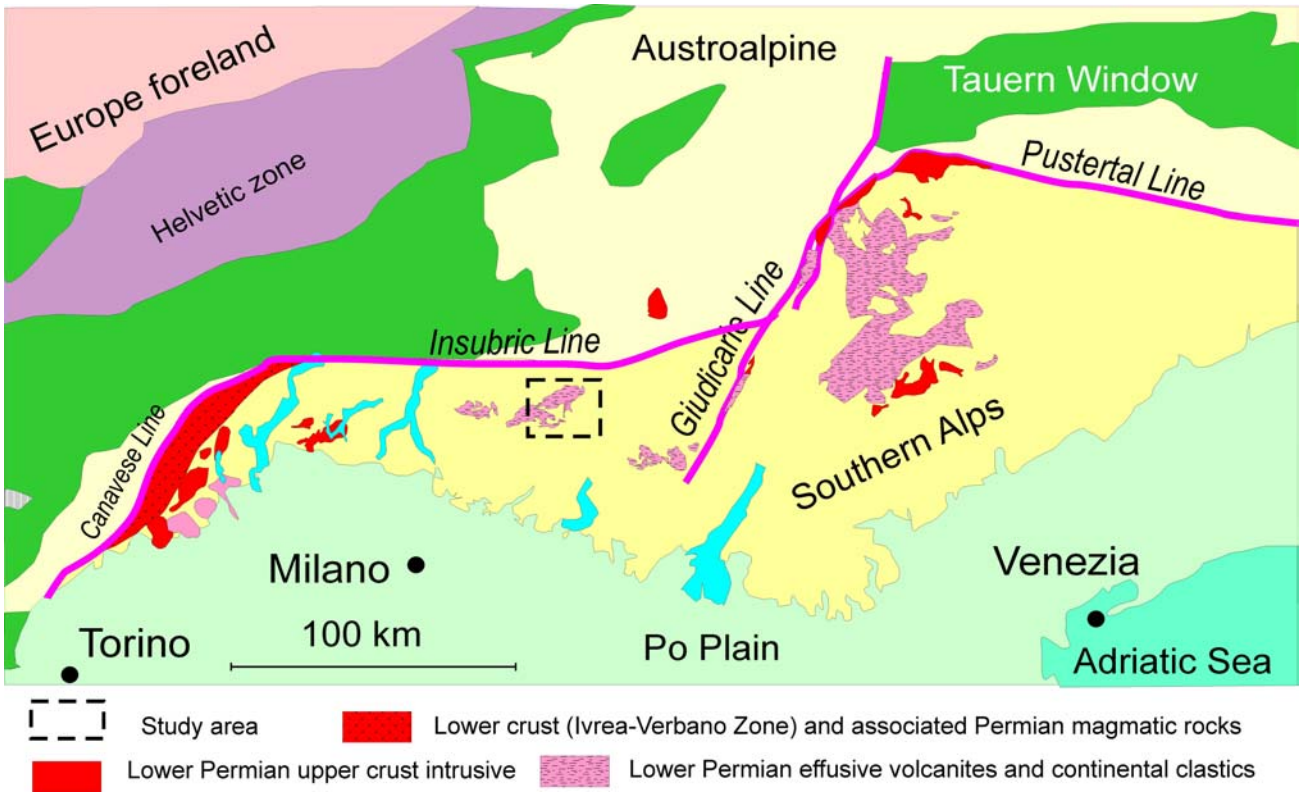

Fig. 1 – Geological setting of the Alpine belt, with the distribution of the Lower Permian sediments and volcanics of the Southern Alps.

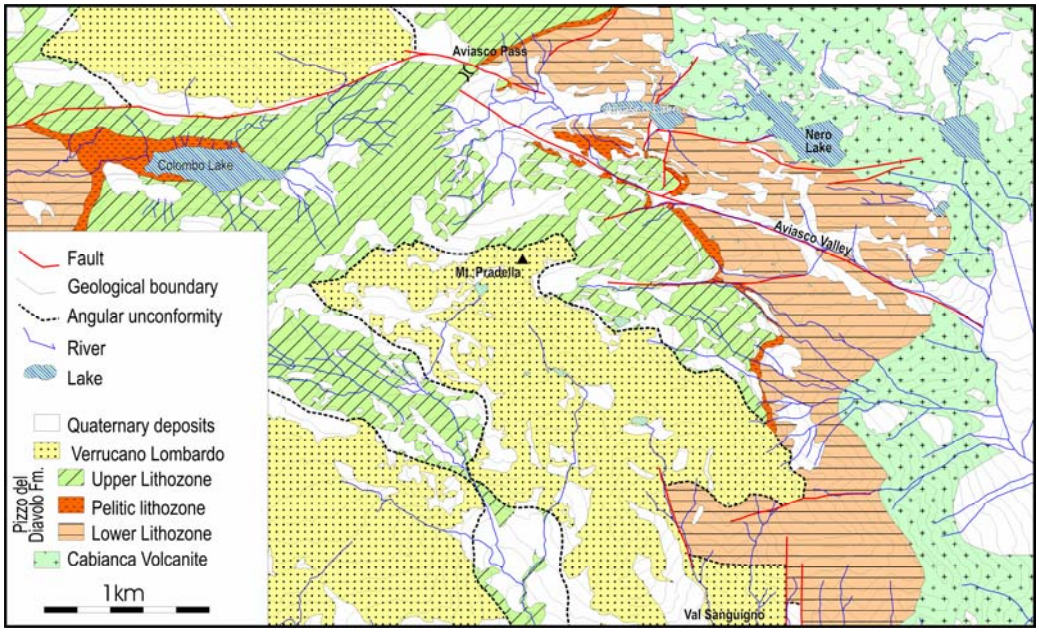

Fig. 2 – Geological map of the study area.

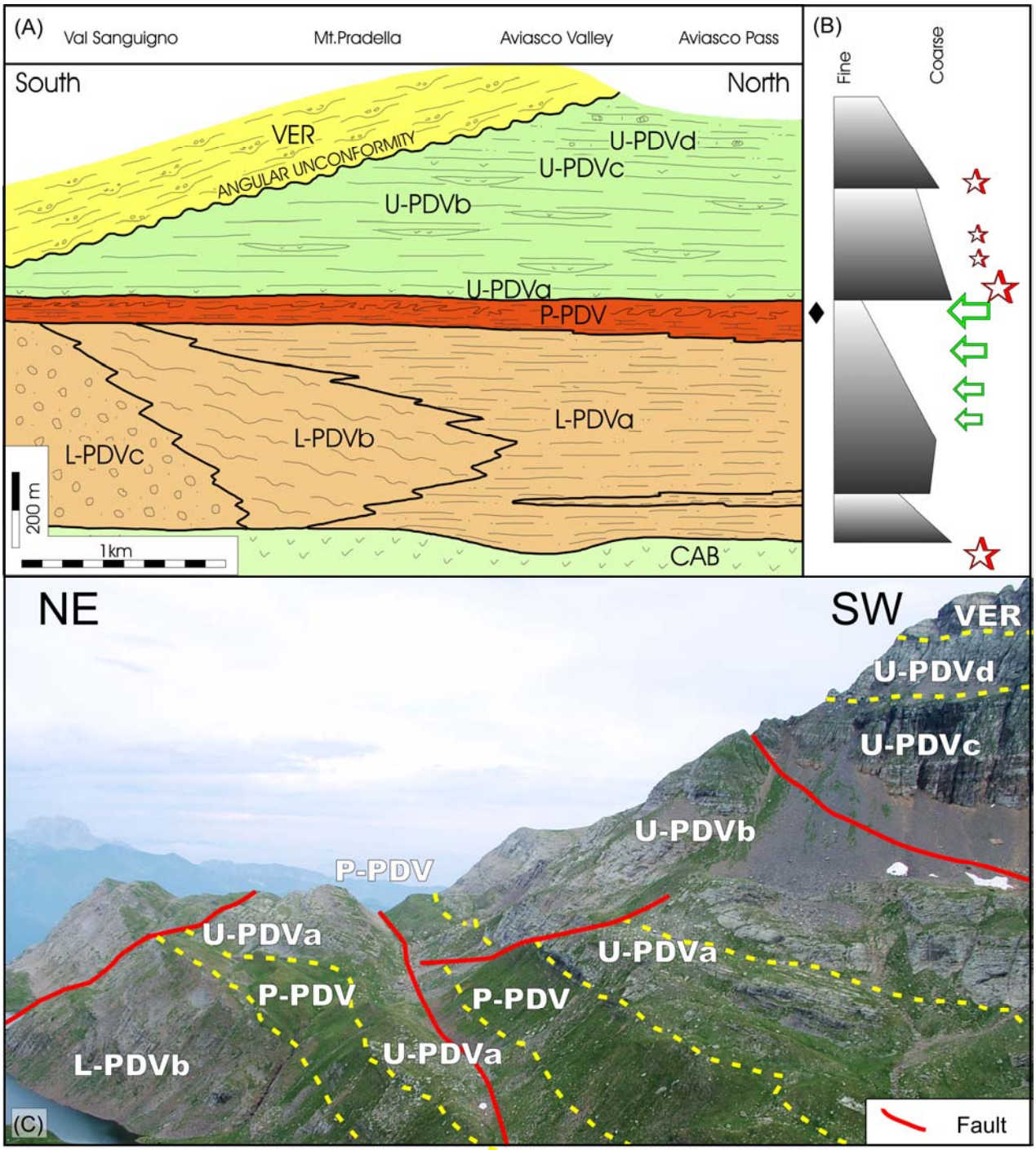

Fig. 3 – (A) Lithostratigraphy of the Permian succession in the study area. The approximate vertical and horizontal scale are represented. Note the polarity of the grain-size distribution in the Lower Lithozone of the Pizzo del Diavolo Formation. On the right (B) the major fining-upward cycles are indicated. Arrows represent the distribution of the soft-sediment deformation and liquefaction structures discussed in the text; stars indicate the major volcanic events. Size of the symbols is qualitatively proportional to the abundance/intensity of the processes. The black diamond indicates the position of the slump in the Pelitic Lithozone. (C) Line drawings from outcrop photograph of the principal Lithozones, near the Aviasco Lake area.

Abbreviations: CAB: Cabianca Vulcanite, prevailing massive ignimbritic flows; L-PDV: Lower Lithozone of the Pizzo del Diavolo Formation; L-PDVa: prevailing bedded, laterally continuous, fine-grained sandstones and siltstones, distal alluvial fan-terminal fan (in this unit, toward the north, a thin pelitic layers with chicken-wire nodules intercalate) ; L-PDVb: prevailing massive sandstone,

with cross-laminations, scoured base and basal lags of clay chips, alluvial fan; L-PDVc: massive conglomerate with volcanic clasts (Val Sanguigno Conglomerate of Cadel et al., 1996), proximal alluvial fan; P-PDV: Pelitic Lithozone of the Pizzo del Diavolo Fm., consisting of siltstones, shales and microbial carbonates. A plurimetric slump is preserved in the middle-upper part of the unit, affecting a bedded alternation of dark siltstones and thin laminated carbonatic beds. Presence of mud cracks, playa-lake environment; U-PVD: Upper Lithozone of the Pizzo del Diavolo Formation; U-PDVa: massive to bedded fine-grained pyroclastic flows; U-PDVb: alternation of prevailing (coarse to fine) sandstones and thin, fine-grained volcanic layers, terminal fan or basin floor; U-PDVc: greenish volcanic flows, very fine-grained; U-PDVd: alternance of fine grained sandstones and siltstones with oncolitic carbonatic layers, up to 0.3 m thick; playa-lake; VER: Verrucano Lombardo, conglomerate and sandstones, braided alluvial plain.

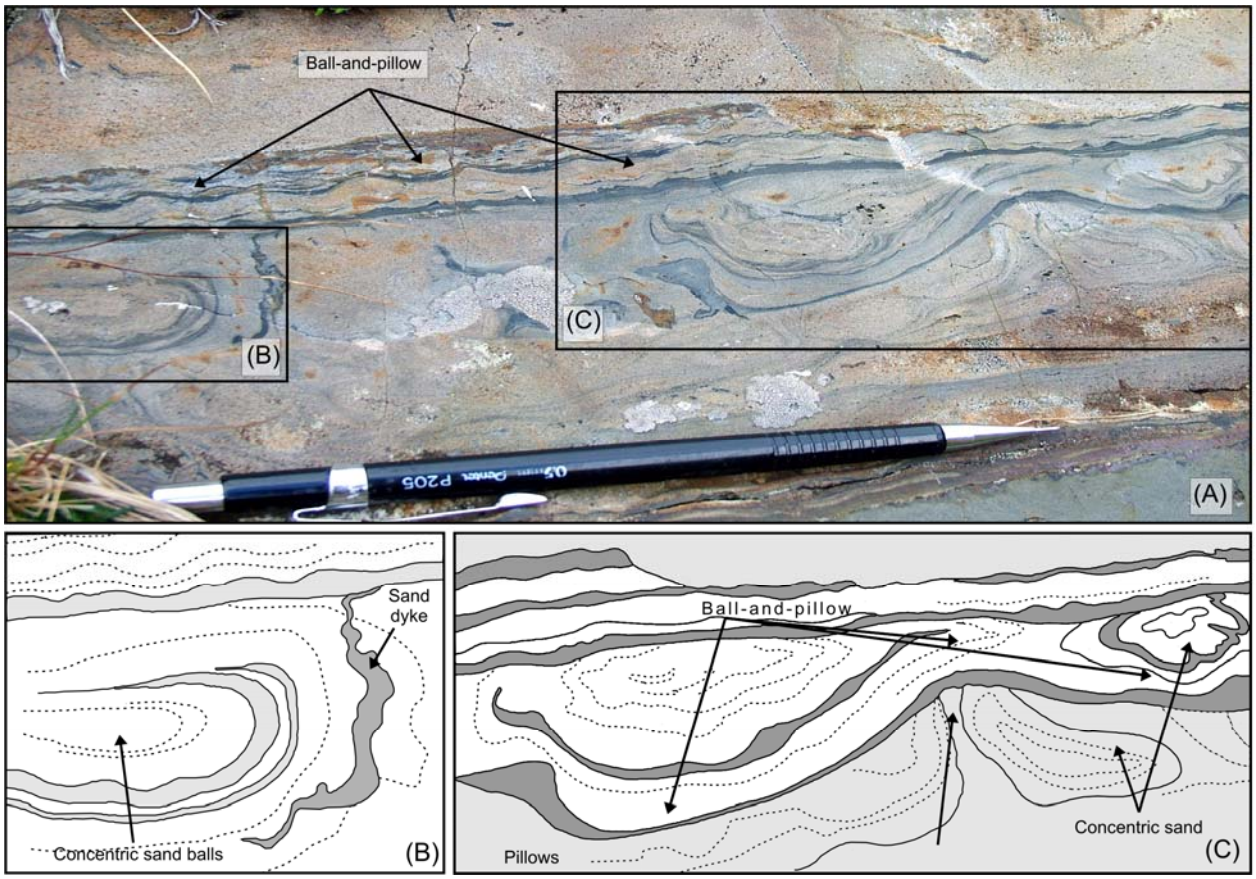

Fig. 4 - Photograph (A) of deformed deposits, illustrating ball-and-pillow structures, surrounded by ripples, that grades into a massive bed. Insets (B) and (C) correspond to line drawings from outcrop photographs: (B) of a ball morphology made of silts and sands; (C) of periodically arranged suites of deformed, concave upward bodies (pillows) and concentric balls.

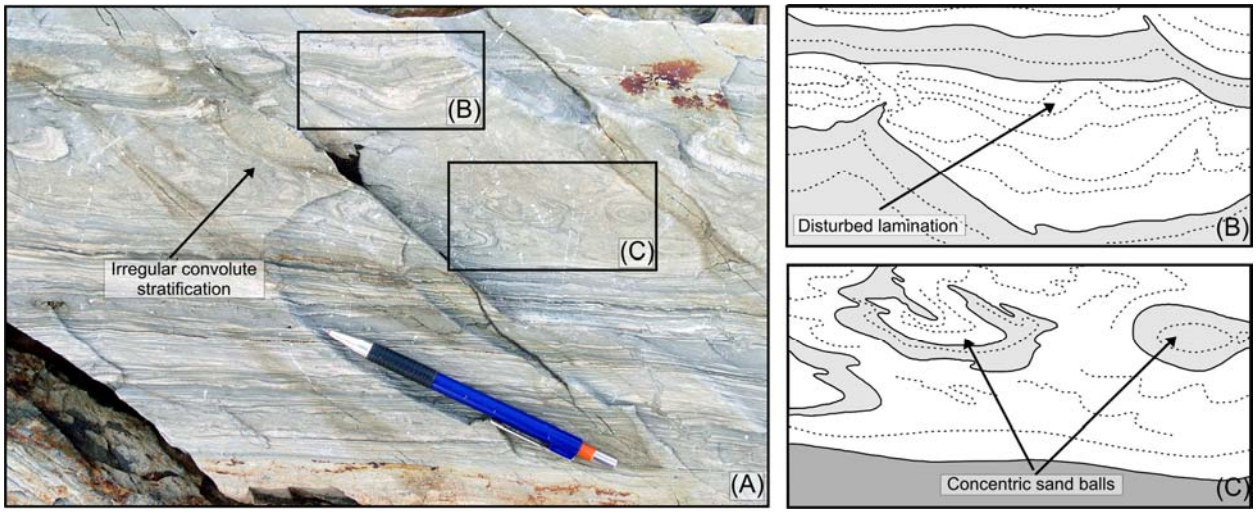

Fig. 5 - (A) irregular convolute deposits sharply overlain by undeformed massive beds. Insets (B) and (C) correspond to line drawings from outcrop photographs: (B) close-up view of disturbed lamination and (C) concentric balls.

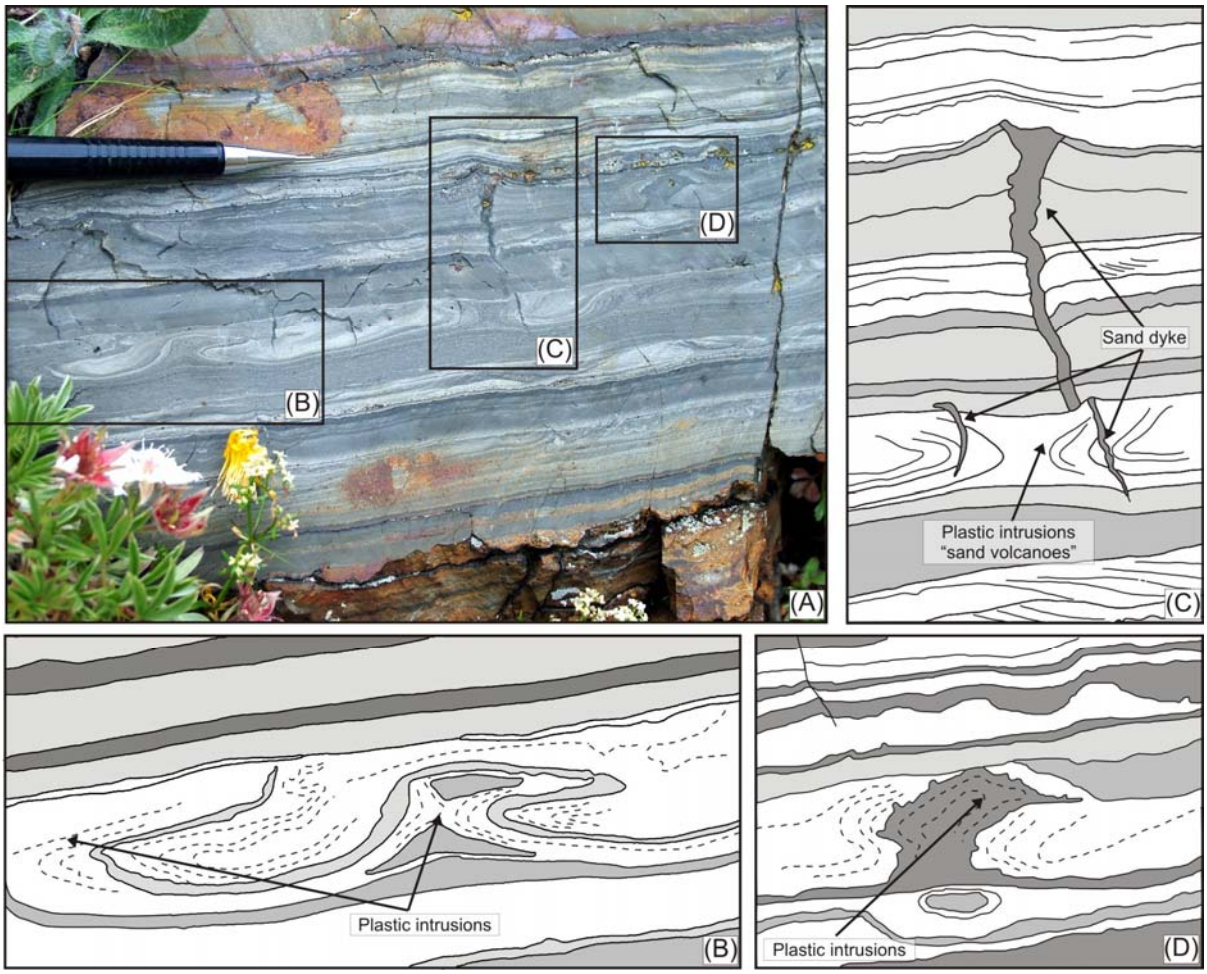

Fig. 6 - (A) Small diapir-like morphologies made of fine material (argillaceous fine sands and silts) which intrudes and deforms overlying beds (laminites). The vergence of the plastic deformations could indicate the existence of low-angle slopes. Insets (B), (C) and (D) correspond to line drawings from outcrop photographs showing plastic intrusions observed at several levels in the lower part of the studied succession. Note also the presence in (C) of a sand dyke, partially cutting the plastic intrusions.

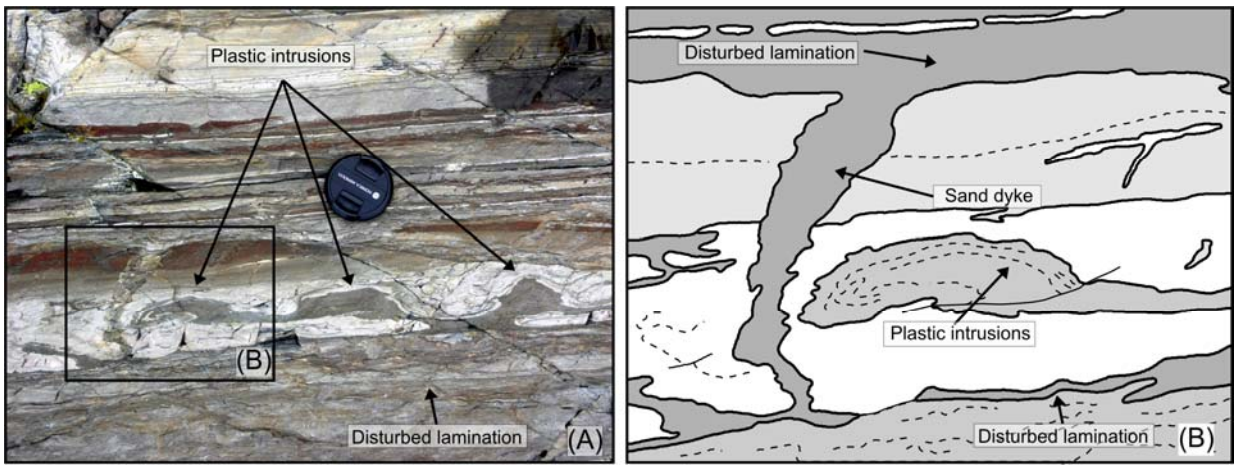

Fig. 7- (A) Plastic intrusion structures due to silts protruding into massive sand. Inset (B) corresponds to line drawings from outcrop photograph of this structures made of fine material (argillaceous fine sands and silts) which intrudes and deforms massive sand. Note also the presence of a sand dyke, cutting the same interval.

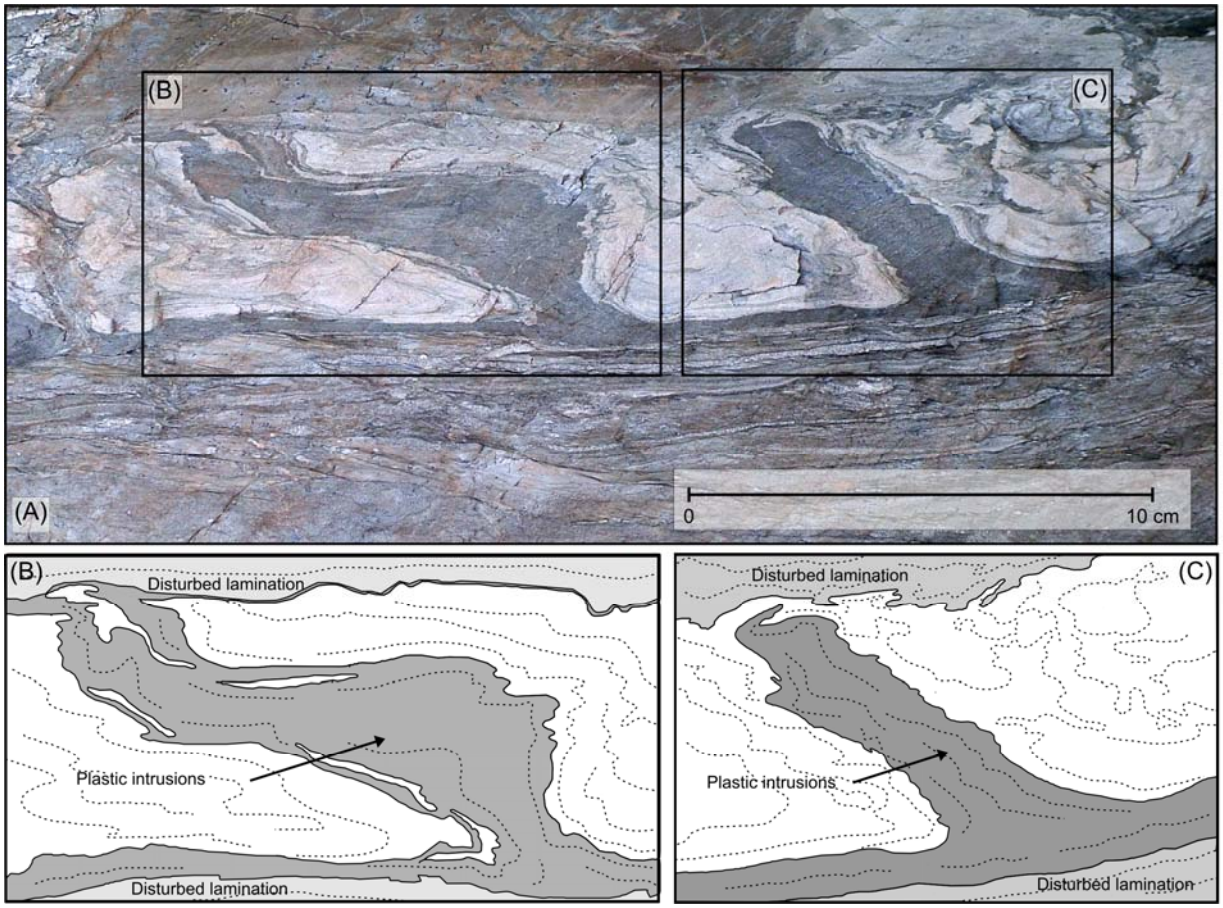

Fig. 8 - (A) Small diapir-like morphologies made of fine material (argillaceous fine sands and silts) which intrudes and deforms massive sand. Bundles of laminae above and below this level display irregular thinning and thickening without losing their lateral geometric continuity (disturbed lamination). Insets (B) and (C) correspond to line drawings from outcrop photographs of plastic intrusions.

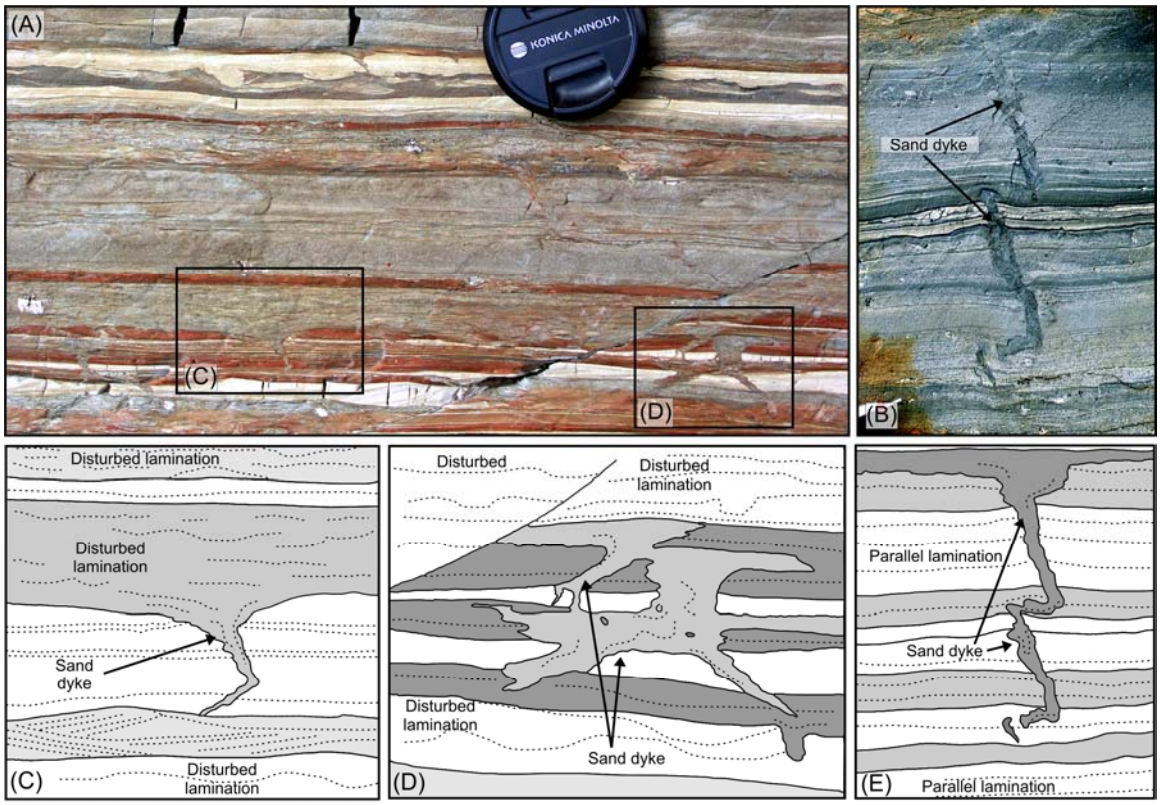

Fig. 9 - (A) Deformed deposits illustrating sand-filled (straight to slightly sinuous in section) fractures, cutting confining horizons of distinct lithologies. These dykes are formed by introduction of material from above. Insets (C), (D) and (E) correspond to line drawings from outcrop photographs of sand-filled (straight to slightly sinuous in section) fractures.

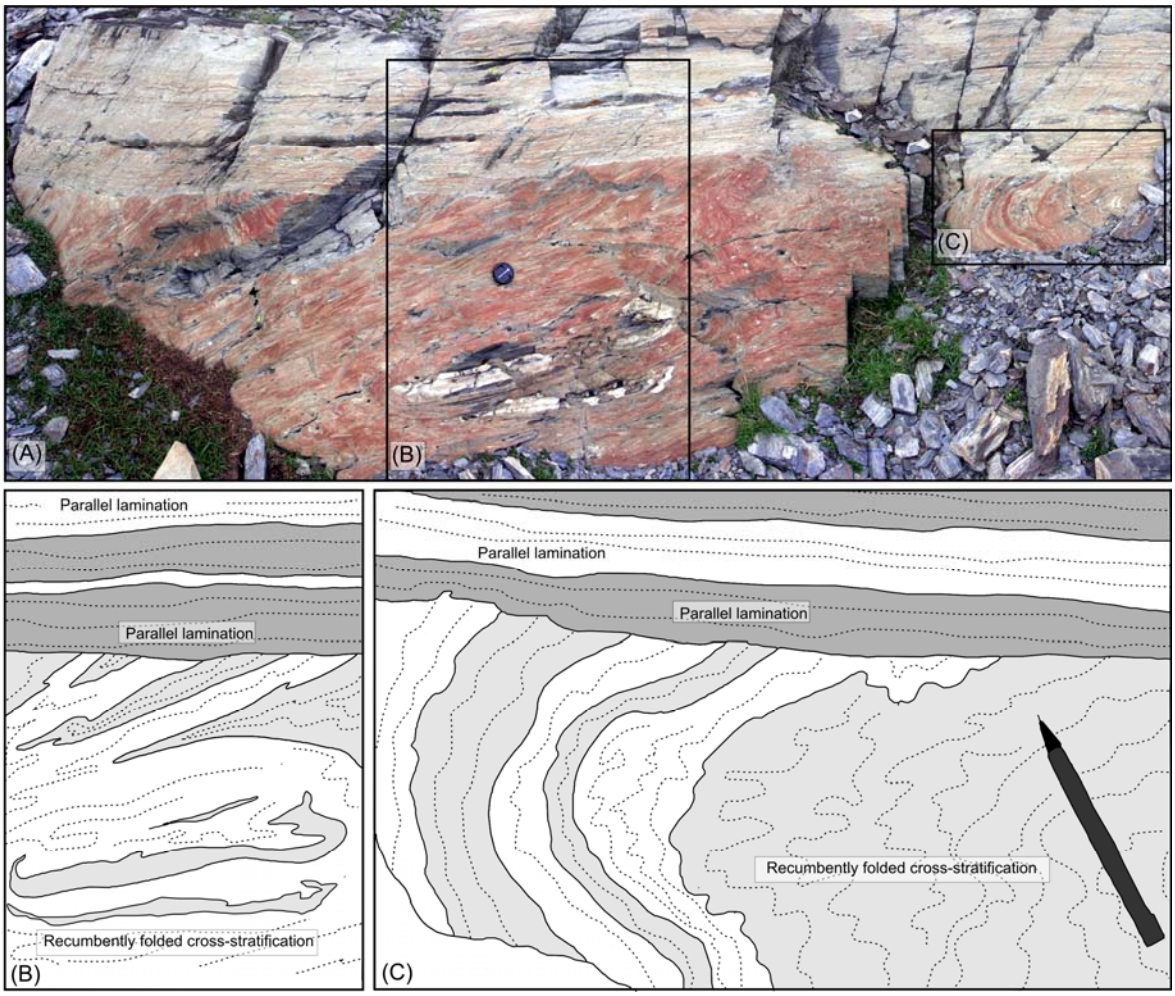

Fig. 10 - (A) Recumbently folded laminations. Examples of deformed beds with overturned internal stratification (like those of classical slumps), which forms recumbent folds with either horizontal or slightly inclined axial planes. Insets (B) and (C) correspond to line drawings from outcrop photographs of recumbently folded laminations.

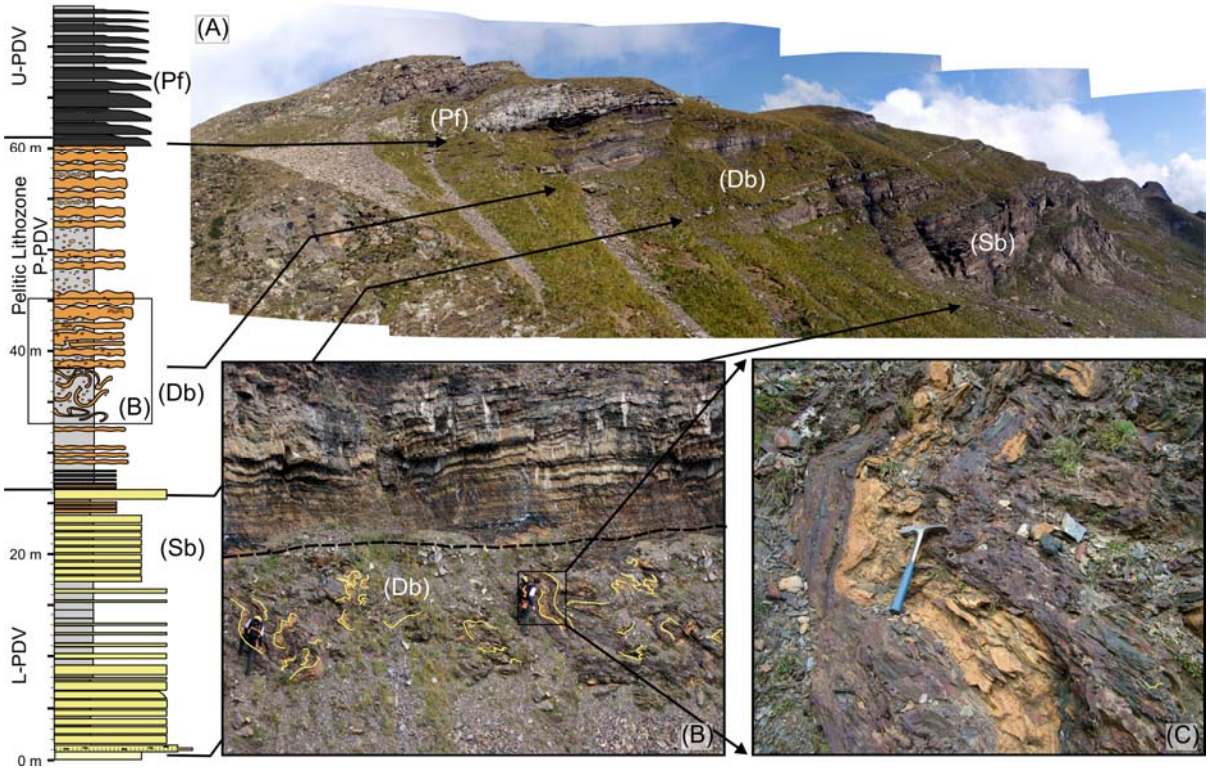

Fig. 11 - (A) Panoramic view (and relative detail log, on the left side) of the thick deformed interval (Db), developed above the prevailing sandstones (Sb) in the Pelitic Lithozone, below the pyroclastic flows (Pf) at the base of the Upper Lithozone (B, C). Recumbently folded cross-stratification is observed within an alternation of dark shales and cm-thick carbonate layers (Pelitic Lithozone). The deformed layer, that can be continuously recognized for about 5 km, is about 4 m thick. The top is sharp and covered by undeformed shales and carbonates. The base is less well defined. The seismite consists of carbonates and shaly layers that are intensely folded. The orientation of the fold axes does not record any vergence.

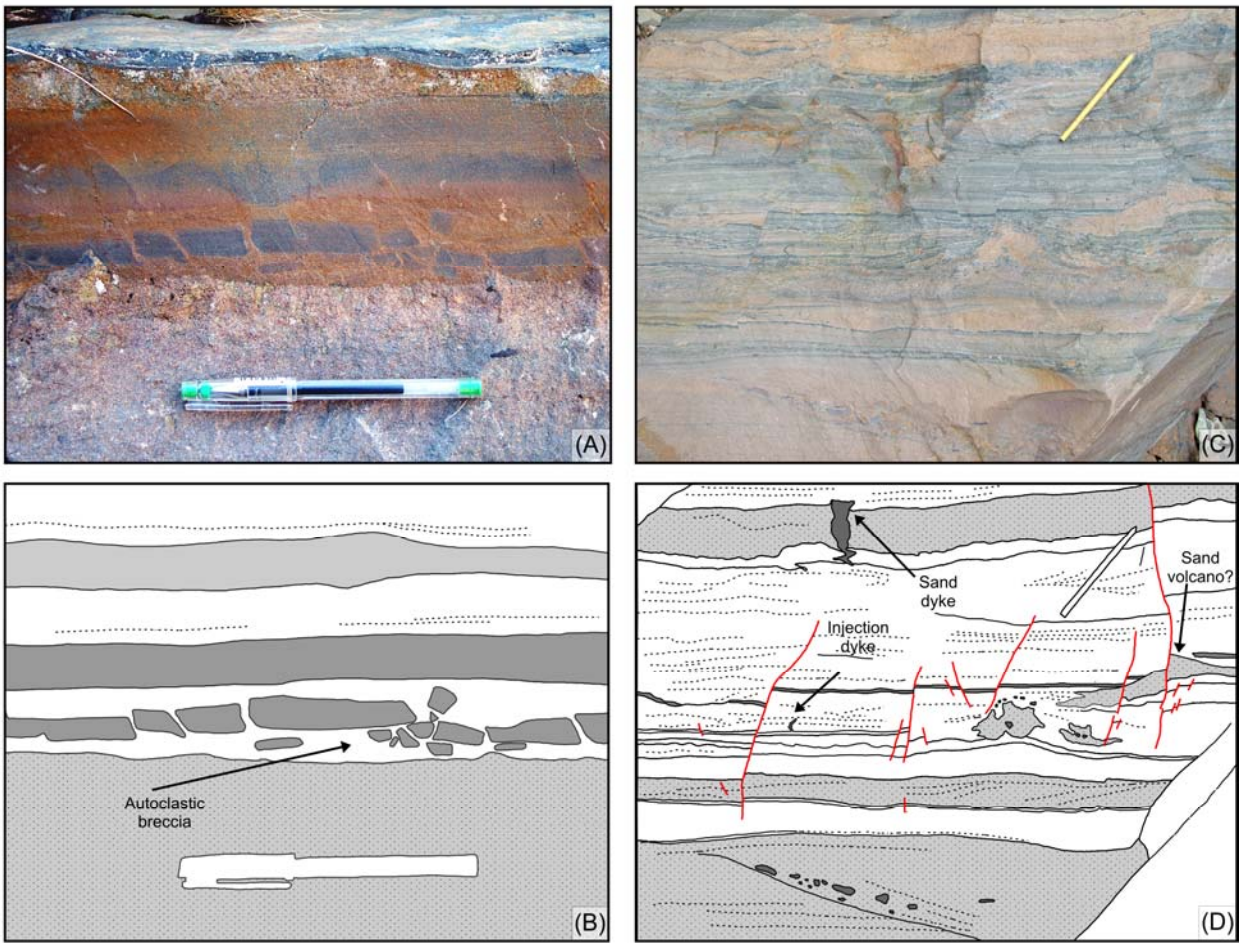

Fig. 12 (A) Autoclastic breccias from fragmentation of indurated fine-grained cohesive silty to fine-grained sand beds. Note the fluidized sand intruded between the breccia clasts. (B) Line drawing of (A). (C) Deformed alternations of laminated siltstones and sandy layers, with evidence of both ductile sediment deformations (liquefaction, disturbed laminations, plastic intrusions) and brittle structures (dykes, normal faults). (D) Line drawing of (C).

	Soft-sediment deformation structure	Description	Mechanism of deformation	Principal trigger mechanisms	Richter magnitude
Ductile deformation structures	***Disturbed lamination, loop-bedded lamination, and mixed layers***	Bundles of laminae that display irregular thinning and thickening without losing their lateral geometric continuity	Low-angle normal micro-faulting	Micro-seismicity	3-5
	Plastic intrusions	Small diapir-like morphologies made of fine material, which intrudes and deforms overlying beds	Liquefaction and/or fluidization processes	Load-induced deformation (rapid deposition) and/or seismic activity	5-6
	Ball-and-pillow structures	Sand bodies with either broad syncline or concentric ball morphology that sink down into sediment of similar composition	Liquefaction and/or fluidization processes	Load-induced deformation (rapid deposition) and/or seismic activity	6-8
	Irregular convolute (or highly distorted) stratification	Highly distorted stratification forming either chaotic patterns or irregular fold that grade into massive bedding	Liquefaction and/or fluidization processes	Load-induced deformation (rapid deposition) and/or seismic activity	6-8
	Recumbently folded cross-stratification (seismoslump)	Cross-stratification forming recumbent folds with horizontal to nearly horizontal axis planes	Liquefaction and/or fluidization processes	Seismic activity	6-8
Brittle deformation structures	***Sand dykes (neptunian dykes and injection dykes)***	Sand-filled fractures, cutting confining horizons of distinct lithologies	Fluidized sediments injected from surrounding strata as a result of increasing interstitial pore pressure	Seismic activity	5-8
	Autoclastic breccias	Brecciation of indurated deposits, commonly represented by cohesive silty or fine-grained sand beds	Brittle deformation penecontempoaneous to deposition. Distinctive of sediments with a high degree of compaction, and thus with under-saturated conditions.	Seismic activity	7-8

Tab. 1 – Mechanism of deformation, trigger mechanisms and possible range of magnitude of the earthquakes related to the observed soft-sediment deformation structures.